Am J Cancer Res 2025;15(9):4067-4081
www.ajcr.us /ISSN:2156-6976/ajcr0168215

Original Article

Deficiency of DAZ genes links testicular germ cell tumorigenesis and infertility: evidence from human embryonic stem cell germline differentiation

Junqing Chen[1,2,3*], Chuyu Li[2,3,4*], Shuangshuang Qiu[3], Wenrui Zhu[3], Xi He[1], Dawei Gao[4], Zifeng Chen[4], Xingli Tong[5], Feiyang Diao[2,3]

[1]Department of Human Anatomy and Histoembryology, Nanjing University of Chinese Medicine, Nanjing 210023, Jiangsu, China; [2]Clinical Center of Reproductive Medicine, First Affiliated Hospital of Nanjing Medical University, Nanjing Medical University, Nanjing 210029, Jiangsu, China; [3]State Key Laboratory of Reproductive Medicine and Offspring Health, Nanjing Medical University, Nanjing 211166, Jiangsu, China; [4]Faculty of Chinese Medicine, Macau University of Science and Technology, Macau 999078, China; [5]Jiangsu Province Hospital of Chinese Medicine, Affiliated Hospital of Nanjing University of Chinese, Nanjing 210000, Jiangsu, China. [*]Equal contributors.

Received August 19, 2025; Accepted September 23, 2025; Epub September 25, 2025; Published September 30, 2025

Abstract: Y-chromosome AZFc deficiency, which includes the DAZ gene family, is one of the most common genetic causes of severe male infertility. Epidemiological and molecular evidence suggest a developmental link between abnormalities in germ cell development and testicular germ cell tumor (TGCT), but whether and how DAZ deficiency is associated with TGCT susceptibility remains unclear. Using a specific human embryonic stem cell (hESC) model, we constructed and characterized a DAZ-deleted cell line (SKLRMe001-A) and compared its efficiency of induction into human primordial germ cell-like cells (hPGCLCs) with that of the H1 control line. We assessed intersections between embryonic-like networks and HMGA1-P53-MAPK/PI3K pathways to explore the potential connection between DAZ deficiency and TGCT susceptibility. DAZ deficiency significantly reduced hPGCLC induction efficiency and downregulated early lineage markers such as SOX17, BLIMP1, and TFAP2C, accompanied by S-phase shortening, cell cycle dysregulation, and increased apoptosis. RNA sequencing and enrichment analyses indicated sustained upregulation of HMGA1 and pointed to dysregulated homeostasis of P53 stress responses and PI3K/AKT and MAPK signaling axes. These findings are consistent with features of TGCT, including maintenance of embryonic-like programs, activation of proliferative signals, and heightened DNA damage responses. Therefore, we propose that lineage differentiation defects and mismatches between stress and survival signaling caused by DAZ deficiency may produce in vivo a population of "undifferentiated and susceptible" cells that increase the risk of TGCT, while also explaining the developmental basis of male infertility. Using a human in vitro model, this study links DAZ deficiency to both infertility and TGCT susceptibility and identifies HMGA1 as a central transcriptional-signaling hub. This finding provides molecular clues for risk stratification and early surveillance in populations with DAZ deficiency and suggests that interventions targeting HMGA1 and the PI3K/AKT and MAPK pathways may simultaneously improve germline differentiation and reduce potential tumor risk.

Keywords: DAZ, AZFc deficiency, primordial germ cells, male infertility, testicular germ cell tumor

Introduction

The development and maintenance of testicular germ cells depend on precise temporal and spatial programmatic regulation [1]. Y chromosome microdeficiencys (YCM) most frequently involve loss of the AZFc region, which contains several gene families critical for spermatogenesis. The DAZ (Deleted in Azoospermia) genes, as important members of the AZFc family, represent the most common molecular defect leading to azoospermia or oligozoospermia [2]. DAZ family proteins are highly conserved RNA-binding proteins that principally exert their physiological functions by binding target RNAs to regulate RNA stability and translation, and

they are widely involved in the regulation of gametogenesis in both sexes [3]. The DAZ family comprises three members: DAZ, DAZL, and BOULE. The DAZL gene is conserved across species and participates in regulating the maintenance and differentiation of germline stem cells; however, the DAZ gene is present only on the Y chromosome from Old World monkeys to humans [4]. Due to the lack of model animals, current functional studies remain at the level of clinical correlation, and no animal models exist to study its function [5].

Concomitant with impaired reproductive function, testicular germ cell tumors (TGCT) - among the most common solid tumors in young adult males - display a distinctive embryonic-like molecular phenotype and developmental origin [6]. Studies indicate that TGCTs, particularly germ cell neoplasia in situ and classical seminoma, arise from aberrant differentiation of fetal or perinatal germ cells, characterized by maintenance of an undifferentiated state, activation of embryonic-like transcriptional networks, and abnormal responses to microenvironmental signals (such as PI3K/AKT, MAPK, and Wnt/β-catenin) [7].

DAZ family proteins play important roles in regulating germ cell development [8]. Loss of DAZL protein in male mice leads to a reduction in spermatogonial numbers, impaired differentiation of spermatogonial stem cells, and only limited progression of spermatocytes to the pachytene stage [9]. More severely, in C57L/B6 mice, DAZL deficiency causes substantial apoptosis of primordial germ cells at embryonic day 15.5, resulting in the absence of germ cells after birth [10]. Recent studies using clinical samples and cancer cell models indicate that DAZ, as a key translational regulator, is essential for maintaining spermatogonial cells. DAZ deficiency may cause proliferative defects of c-KIT-positive spermatogonia and spermatogenic failure in AZFc-deleted patients [11]. Irregular proliferation and sustained pluripotency of human primordial germ cells (hPGCs) are associated with testicular tumors and ovarian cancer [12]. However, because of the lack of experimental models, the expression of DAZ at specific stages of spermatogenesis and the associated molecular mechanisms remain unclear.

In vitro gametogenesis from pluripotent stem cells offers a model to elucidate mechanisms of germ cell development [13, 14]. Human pluripotent stem cells can be induced into human primordial germ cell-like cells (hPGCLCs) [15-17]. In this study, we utilized a DAZ-deficient human embryonic stem cells (hESC) line (SKLRMe001-A), derived from an embryo donated by a patient clinically diagnosed with AZFc deficiency [18]. By directing differentiation of this cell line and of a normal male hESC line (H1) into hPGCLCs, we compared the differentiation efficiency, the differentiation process, and characteristics of the differentiated cells between the two groups. During induction of SKLRMe001-A cells into hPGCLCs, colonies were looser in structure and apoptotic cells increased. BLIMP1, TFAP2C, and SOX17 are key factors in early hPGC specification [19]. Compared with H1 cells, DAZ-deficient cells exhibited differences in expression of pluripotency markers and reduced expression levels of early germ cell markers. Additionally, DAZ-deficient cells showed shortened S phase, cell cycle arrest, and increased apoptosis. Transcriptomic and bioinformatics analyses revealed upregulation of the transcription factor HMGA1. We further used the TRRUST online transcriptional regulatory analysis tool to predict and analyze potential upstream regulators of HMGA1 and downstream target genes that HMGA1 might regulate. E2F1 and MYCN were jointly identified as two putative activators/regulators of HMGA1, and downstream genes potentially directly regulated by HMGA1 included one activated gene (P53) and four repressed genes (BRCA1, CDH1, INSR, and XPA). These key upstream and downstream genes provide new directions for understanding HMGA1's regulatory role in early spermatogonial differentiation defects. We hypothesize that when DAZ deficiency leads to aberrant overexpression of HMGA1, it activates the P53 gene and, via downstream MAPK/PI3K signaling pathways, induces abnormal apoptosis and cell cycle perturbations, ultimately causing early spermatogenic failure. However, the specific mechanisms and the actual upstream and downstream regulatory pathways require further analysis and exploration.

Methods and materials

Cell culture

Human embryonic stem cells (hESCs) were established on the feeder layer system in the 4:1 medium [20% knockout serum replace-

ment (Gibco, Grand Island, USA), 1% MEM non-essential amino acid solution (Gibco), 1% penicillin and streptomycin, 2 mM L-glutamine, and 0.1 mM 2-mercaptoethanol in DMEM/F12 (Gibco)] supplemented with 2 ng/ml bFGF (R&D Systems, Minneapolis, USA). hESCs were maintained using a feeder-free culture system. The culture medium consisted of mTeSR2 (STEMCELL Technologies, Vancouver, Canada), a defined, serum-free medium specifically formulated to support the undifferentiated growth of human embryonic and induced pluripotent stem cells. Cells were cultured in a controlled environment using a humidified CO_2 incubator maintained at 37°C with 5% CO_2. Cells were typically passaged every 3-5 days when reaching approximately 70-80% confluence to prevent over-confluence, which can lead to spontaneous differentiation or reduced viability.

Induction and expansion of hPGCLCs

In vitro differentiation of human primordial germ cell-like cells (hPGCLCs) was performed through an intermediate mesoderm-like cell (iMeLCs) stage, following established protocols with modifications [15]. Briefly, iMeLCs were induced from hESCs (2.5×10^5 cells/well) in the GK15 medium [15% knockout serum replacement (Gibco), 1% MEM non-essential amino acid solution (Gibco), 1% penicillin and streptomycin, 2 mM L-glutamine, 2 mM sodium pyruvate (Gibco), and 0.1 mM 2-mercaptoethanol in GMEM (Gibco)] supplemented with 100 ng/ml Wnt3a (R&D Systems), 50 ng/ml Activin A (R&D Systems), and 10 μM Y-27632 (MCE, Shanghai, China) on a fibronectin (Sigma, St. Louis, USA)-coated 12-well plate (the induction time was 44-48 h for hESCs). hPGCLCs were induced from iMeLCs (3.0×10^3 cells/ well) in the GK15 medium supplemented with 200 ng/ml BMP4 (R&D Systems), 100 ng/ml SCF (R&D Systems), 20 ng/ml LIF (R&D Systems), 50 ng/ml EGF (R&D Systems), and 10 μM Y-27632 in a V-bottom 96-well plate (Thermo, Grand Island, USA). After 6 days from hPGCLCs induction, hPGCLCs were isolated by FACS sorting [see the Fluorescence-activated cell sorting (FACS) section]. Phase-contrast images of hESCs and iMeLCs were acquired using a Nikon ECLIPSE Ts2 inverted microscope equipped with a DS-Fi2 camera. iMeLCs aggregates during hPGCLCs induction were documented using a Nikon ECLIPSE Ts2R-FL inverted microscope with DS-Fi2 camera. Following established protocols with modifications, hPGC LCs (1×10^5 cells/well) were expanded on the 6-well plate coated with m220 cells in adv RPMI medium (Gibco) containing 2.5% FBS (Gibco) supplemented with 100 ng/ml SCF, 10 ng/ml LIF, 50 ng/ml EGF, 20 ng/ml bFGF, 25 ng/ml BMP2 (R&D Systems), 10 μM forskolin (Sigma), 10 μM rolipram (Sigma), and passaged every 10 days [16, 17].

Flow cytometry and cell sorting

Human primordial germ cell-like cells were generated through an optimized differentiation protocol beginning with iMeLCs aggregates that underwent PBS washing followed by enzymatic dissociation using a 1:1 mixture of 0.5% trypsin-EDTA (Gibco) and PBS at 37°C for 15 minutes, with mechanical dispersion achieved through pipetting before neutralization using supplemented DMEM (Gibco) containing 10% FBS, antibiotics, 2 mM L-glutamine, 10 μM Y-27632, and 0.1 mg/ml DNase I (Gibco). The pelleted cells were resuspended in FACS buffer (PBS with 0.1% BSA and Y-27632), filtered through a 40 μm strainer (Thermo), then stained with BV421-conjugated anti-CD49f (Bio Legend, San Diego, USA) and APC-conjugated anti-CD326 (Bio Legend) on ice for 15 minutes protected from light before washing and final filtration. Cell populations were sorted based on CD49f and EpCAM expression profiles using a FACSAria III (BD Biosciences, San Jose, USA), with cells collected either in FACS buffer for culture or downstream applications including RT-qPCR, RNA-seq. After removing cellular clumps with Falcon Cell Strainer, the cells were subjected to FACS sorting. To analyze the expression of pluripotency surface marker in hESCs, the cells suspended in FACS buffer were incubated with anti-TRA-1-81 antibody (Thermo) on ice for 30 min in the dark and washed with PBS once. After pelleting, the cells were resuspended in FACS buffer, filtered through a Falcon Cell Strainer, and analyzed by flow cytometry.

Immunofluorescence staining

Cells were fixed with 4% paraformaldehyde (Sigma). For permeabilization, cells were treated with 0.1% Triton X-100 in PBS for 10 minutes at room temperature. Non-specific binding sites were blocked using blocking buffer containing 1% bovine serum albumin (Sigma), and stained

Table 1. Primer sequences

Gene	Primer Sequences
OCT4-F	5'-CTGTCTCCGTCACCACTCTG-3'
OCT4-R	5'-AAACCCTGGCACAAACTCCA-3'
NANOG-F	5'-AGAGGTCTCGTATTTGCTGCAT-3'
NANOG-R	5'-AAACACTCGGTGAAATCAGGGT-3'
SOX2-F	5'-TGAATCAGTCTGCCGAGAATCC-3'
SOX2-F	5'-TCTCAAACTGTGCATAATGGAGT-3'
BLIMP1-F	5'-AAACCAAAGCATCACGTTGACA-3'
BLIMP1-R	5'-GGATGGATGGTGAGAGAAGCAA-3'
TFAP2C-F	5'-ATTAAGAGGATGCTGGGCTCTG-3'
TFAP2C-R	5'-CACTGTACTGCACACTCACCTT-3'
NANOS3-F	5'-TGGCAAGGGAAGAGCTGAAATC-3'
NANOS3-R	5'-TTATTGAGGGCTGACTGGATGC-3'
SOX17-F	5'-TTCGTGTGCAAGCCTGAGAT-3'
SOX17-R	5'-TAATATACCGCGGAGCTGGC-3'
DPPA3-F	5'-AAGCCCAAAGTCAGTGAGATGA-3'
DPPA3-R	5'-GCTATAGCCCAACTACCTAATGC-3'
DDX4-F	5'-TCATACTTGCAGGACGAGATTTG-3'
DDX4-R	5'-AACGACTGGCAGTTATTCCATC-3'
DAZL-F	5'-ATGTTGTACCTCCGGCTTATTCA-3'
DAZL-R	5'-CCATTTCCAGAGGGTGGAGTA-3'
PLZF-F	5'-CCTCAGACGACAATGACACGG-3'
PLZF-R	5'-CTCGCTGGAATGCTTCGAGAT-3'
GAPDH-F	5'-GGAGCGAGATCCCTCCAAAAT-3'
GAPDH-R	5'-GGCTGTTGTCATACTTCTCATGG-3'
ARBP-F	5'-GAAACTCTGCATTCTCGCTTCC-3'
ARBP-R	5'-ACTCGTTTGTACCCGTTGATGA-3'

with antibodies against OCT4 (Abcam, Cambridge, UK), Nanog (Abcam), SSEA4 (Abcam), Tra-1-60 (Abcam), DAZL (Abcam), BLIMP1 (R&D Systems), TFAP2C (Santa Cruz, Dallas, USA), SOX17 (Neuromics, Edina, USA). Nuclear counterstaining was performed with DAPI. Images were captured using a confocal microscope.

Quantitative RT-qPCR

Total RNA was extracted using TRIzol reagent (TIANGEN, Beijing, China), and cDNA was synthesized using a reverse transcription kit (Promega, Madison, USA) following the manufacturer's instructions. qPCR was performed using SYBR Green master mix (Thermo) and primers specific for germ cell markers, and other genes of interest. The relevant gene sequences were retrieved from the NCBI database, and primer sequences were subsequently designed using Primer-BLAST. The specific primer sequences are shown in **Table 1**. Expression levels were normalized to GAPDH.

Crystal violet staining

After 24 hours of cell seeding in culture dishes, cells were washed three times with DPBS. The cells were then immersed in crystal violet staining solution for 10 minutes (Beyotime, C0121). Following staining, the samples were thoroughly washed with distilled water to remove excess staining solution. Observation and photography were performed under a microscope.

RNA sequencing and bioinformatics analysis

RNA-seq was performed on H1 and SKLRMe-001-A cells at different stages of hPGCLC differentiation. Library preparation and sequencing were conducted on the Illumina platform. Differentially expressed genes were identified using DESeq2, and pathway enrichment analysis was performed using KEGG and GO databases. The TRRUST database was used to predict transcription factor networks.

Apoptosis assay

Apoptosis detection in thyroid cells from each experimental group was performed using the TUNEL BrightRed Apoptosis Detection Kit (Vazyme, A113) following the manufacturer's protocol. The assay was conducted on paraffin-embedded tissue sections according to standard TUNEL methodology. Fluorescence microscopy analysis was carried out using a Zeiss fluorescence microscope (Zeiss AG, Oberkochen, Germany), with detection of Bright Red fluorescence at 620±20 nm and DAPI nuclear counterstaining at 460 nm through appropriate filter sets. Quantification of apoptotic cells within tissue sections was independently performed by two technicians in a blinded manner to ensure objective assessment.

Statistical analysis

Data were presented as mean ± SEM from at least three independent experiments. Statistical analyses were performed using GraphPad Prism software. Student's t-test was used for comparing two groups, and one-way ANOVA with Tukey's post-hoc test was used for multiple group comparisons. $P < 0.05$ was considered statistically significant.

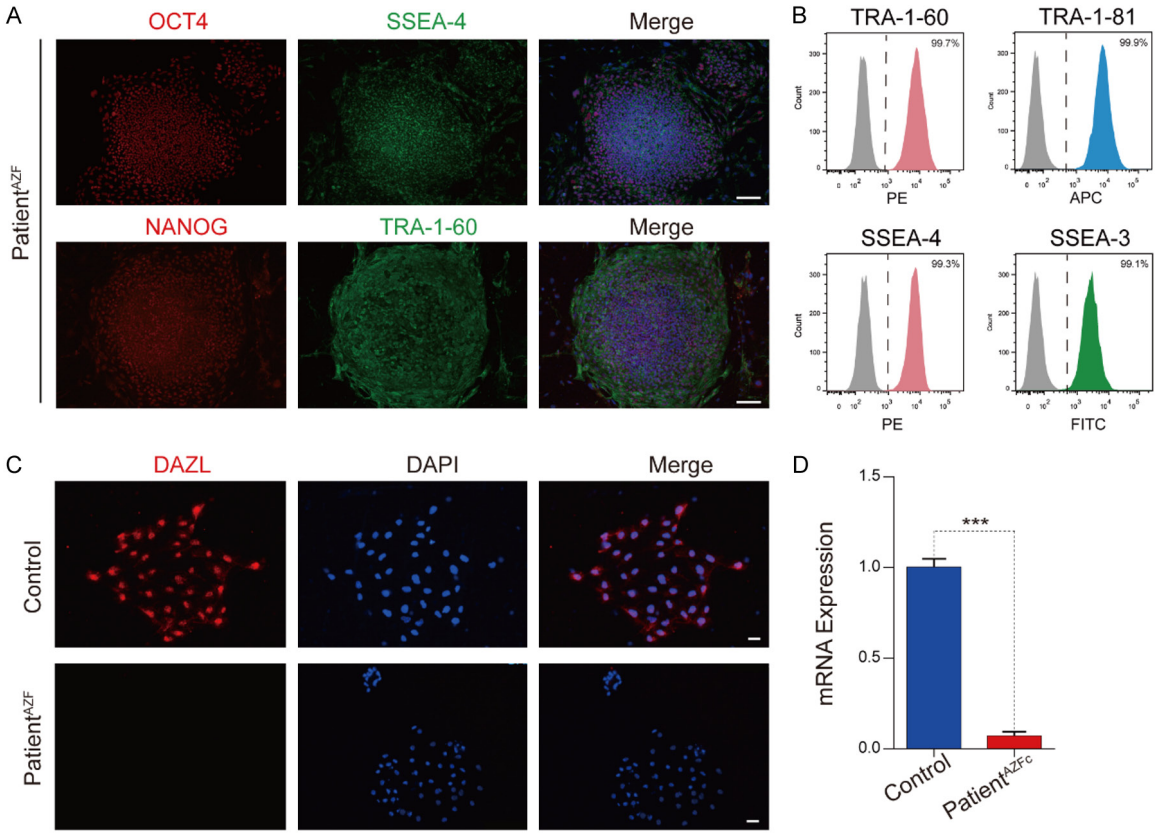

Figure 1. Deficiency of the DAZL gene in the human Embryonic Stem Cell line SKLRMe001-A. A. Immunofluorescence analyses of OCT4, NANOG, SSEA-4, TRA-1-60 gene expression in SKLRMe001-A hESCs (PatientAZFc). The DNA was stained with DAPI. Scale bar, 50 μm. B. Flow cytometric analysis of TRA-1-60 (PE), TRA-1-81 (APC), SSEA-4 (PE), and SSEA-3 (FITC) expression in SKLRMe001-A hESCs with isotype controls (Gray). Quantification of positive cells > 95% of cells expressed TRA-1-60 and SSEA-4, confirming pluripotency. C. Representative immunofluorescence images of H1 hESCs (Control) and SKLRMe001-A hESCs (PatientAZFc) stained for DAZL (Red) and DAPI for nuclei (Blue). Scale bar, 10 μm. D. Relative DAZL mRNA expression levels in H1 hESCs (Control) versus SKLRMe001-A hESCs (PatientAZFc), normalized to GAPDH and calculated by 2-ΔΔCt. Control expression was defined as 1 (Left). Data represent mean ± SEM (n = 3 independent differentiation experiments, each with triplicate qPCR measurements). ***P < 0.001 by unpaired t-test.

Results

Deficiency of the DAZL gene in the human embryonic stem cell line SKLRMe001-A

To validate the quality and pluripotent characteristics of the human embryonic stem cell line SKLRMe001-A utilized in this study, flow cytometric analysis was conducted to determine the expression levels of pluripotency-associated surface markers in cultured SKLRMe001-A cells. Flow cytometry results demonstrated robust expression of key pluripotency markers including TRA-1-81, Tra-1-60, SSEA-3, and SSEA-4, confirming that the SKLRMe001-A cell line retained its undifferentiated pluripotent characteristics throughout culture (**Figure 1A**).

To provide additional validation of pluripotency, immunofluorescence microscopy was performed to examine the expression and subcellular localization of critical transcription factors OCT4 and Nanog. Immunofluorescence analysis revealed distinct nuclear localization and strong expression of both OCT4 and Nanog, further substantiating that SKLRMe001-A cells maintained expression of essential pluripotency regulators in their appropriate cellular compartments (**Figure 1B**).

Additionally, we confirmed the absence of DAZ expression in SKLRMe001-A cells compared to the normal male H1 hESC line by qPCR and immunofluorescence, providing important baseline characterization for subsequent experimental comparisons (**Figure 1C**, **1D**).

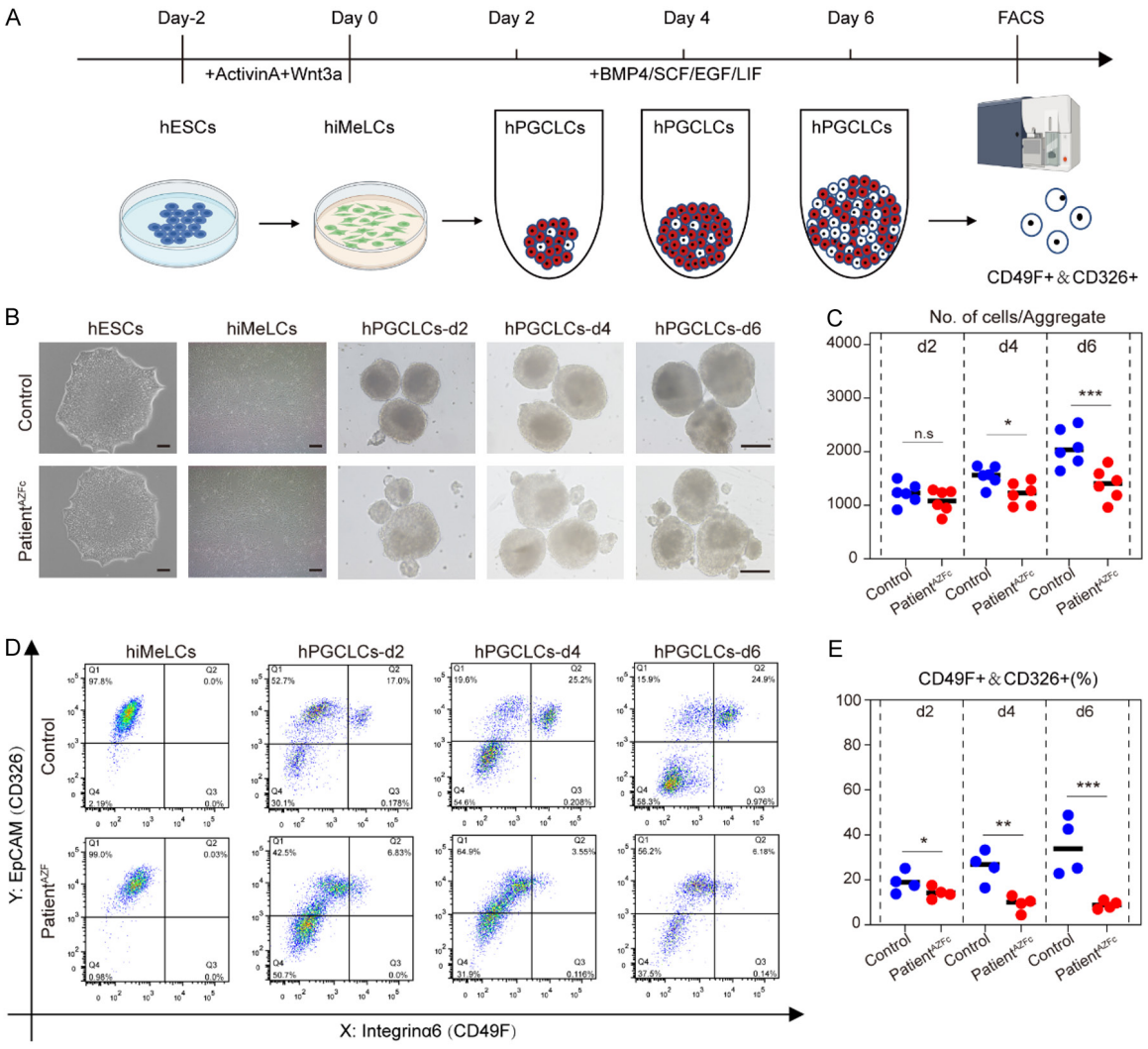

Figure 2. DAZ deficiency impairs hPGCLCs differentiation efficiency. A. Stepwise Differentiation and Purification of hPGCLCs from hESCs. Schematic of the 6-day protocol: hESCs (Day -2) to hiMeLCs (Day 0, Activin A/Wnt3a) and hiMeLCs to hPGCLCs (Days 2-6, BMP4/SCF/EGF/LIF). B. Bright-field (BF) images of undifferentiated hESCs (feeder free) and iMeLCs (epiblast-like monolayer) at Day -2 and Day 0, respectively. Scale bars: 50 μm; BF images of floating hPGCLCs aggregates (3,000 cells/initial aggregate) at Day 2/4/6 in Control vs. PatientAZFc groups. Scale bars: 200 μm. C. Cell numbers per aggregate for control (blue) and PatientAZFc (red) groups. Data are from 6 independent experiments (≥ 5 aggregates/group). Mean values are shown as bars. n.s (not significant), $P > 0.05$, *$P < 0.05$, ***$P < 0.001$ by unpaired t-test. D. Flow cytometric analysis of EPCAM (CD326) and Integrin-α6 (CD49F) expression during hiPSCs-to-hPGCLCs differentiation in Control and PatientAZFc groups. Quantification of CD326+ and CD49F+ cells (Q4 quadrant) in Control vs PatientAZFc groups. E. Percentage of CD326+ and CD49+ cells (Q4 quadrant) in control (blue) and PatientAZFc (red) groups. Data are from 4 independent experiments. Mean values are shown as bars. *$P < 0.05$, **$P < 0.01$, ***$P < 0.001$ by unpaired t-test.

DAZ deficiency impairs hPGCLCs differentiation efficiency

To elucidate the functional role of DAZ in human germ cell development, we employed established differentiation protocols to induce both cell lines toward human primordial germ cell-like cells (hPGCLCs). Primed human induced pluripotent stem cells (hiPSCs) were first cultured under serum-free conditions and differentiated into incipient mesoderm-like cells (iMeLCs), which subsequently underwent further specification into hPGCLCs following previously validated protocols (**Figure 2A**).

Morphological assessment by light microscopy during the differentiation process revealed distinct phenotypic differences between the two

cell lines. Normal H1 cells undergoing hPGCLCs induction formed characteristic dense, compact cell clusters with well-defined boundaries and uniform morphology. In contrast, AZFc-deleted stem cells exhibited compromised differentiation capacity, characterized by the presence of cellular debris, loosely organized cell aggregates, and marked heterogeneity in cluster size and cell number (**Figure 2B** and **2C**).

Following a 6-day induction period, cells were harvested and subjected to fluorescence-activated cell sorting (FACS) analysis to quantitatively assess and compare the differentiation efficiency between the two experimental groups. EpCAM and integrin α6 were used as specific surface markers for hPGCLC specification. The proportion of $EpCAM^+$/Integrin $\alpha6^+$ double-positive cells in control H1 cells reached 24.9%, substantially exceeding the 6.18% observed in SKLRMe001-A cells at day 6 (**Figure 2D**). Repeated experiments consistently showed that the differentiation efficiency of AZFc-deficient cell lines was significantly reduced at day 6 (**Figure 2E**). This marked decrease in hPGCLCs induction efficiency demonstrates the critical requirement of the AZFc region for proper human germ cell specification and development.

DAZ deficiency impairs critical transcription factor expression during hPGCLCs specification

To characterize the primordial germ cell identity of the induced hPGCLCs, immunofluorescence microscopy was performed to evaluate the expression and subcellular localization of key germ cell specification markers. Cells undergoing hPGCLCs differentiation were fixed and processed for immunofluorescence staining at specific time points during the induction process.

Immunofluorescence analysis revealed robust expression of essential early primordial germ cell markers as early as day 4 post-induction, indicating successful initiation of germ cell specification. Triple immunofluorescence staining demonstrated concurrent expression and nuclear co-localization of critical transcription factors including Ap2γ (TFAP2C), SOX17, and BLIMP1 (PRDM1). This coordinated expression pattern of the core germ cell regulatory network confirmed that the differentiated cells had acquired authentic primordial germ cell characteristics and were progressing through the appropriate developmental program.

Immunofluorescence staining demonstrated that while H1-derived hPGCLCs exhibited robust expression of SOX17, BLIMP1, and TFAP2C, SKLRMe001-A-derived cells showed markedly reduced expression of these markers, confirming impaired germ cell specification in the absence of DAZ (**Figure 3A**).

qPCR analysis further confirmed decreased expression of key primordial germ cell markers, including SOX17, BLIMP1, and TFAP2C, in DAZ-deficient cells (**Figure 3B**).

DAZ deficiency induces apoptosis in hPGCLCs differentiation and inhibits hPGCLCs expansion in vitro

Cell cycle analysis revealed that DAZ-deficient cells exhibited abnormal cell cycle distribution during hPGCLCs differentiation, characterized by shortened S phase, delayed G0/G1 and G2/M phases (**Figure 4A**, **4B**). This suggested that DAZ deficiency disrupts cell cycle progression during germ cell specification.

Furthermore, TUNEL staining confirmed elevated apoptotic rates in DAZ-deficient cells (**Figure 4C**, **4D**). These findings indicate that DAZ deficiency leads to cell cycle abnormalities and increased apoptosis during hPGCLCs differentiation.

To assess the in vitro expansion of DAZ-deficient hPGCLCs, we cultured them on m220 feeders alongside controls (**Figure 4E**). Unexpectedly, DAZ-deficient hPGCLCs demonstrated enhanced clonogenicity, forming more colonies than controls (**Figure 4F-H**). Morphologically, the groups differed profoundly. Control cells exhibited a spindle-shaped, loose colony morphology with oval nuclei and prominent perinuclear chromatoid bodies, consistent with germ cell identity. In contrast, DAZ-deficient colonies resembled hESCs, forming compact, dome-shaped clusters with defined borders (**Figure 4I**). Flow cytometry for key markers confirmed this phenotypic shift. Notably, 70.1% of DAZ-deficient cells were EPCAM+ Integrin-α6-, a profile indicative of dedifferentiation. Conversely, the EPCAM+ Integrin-α6+ population - a hall-

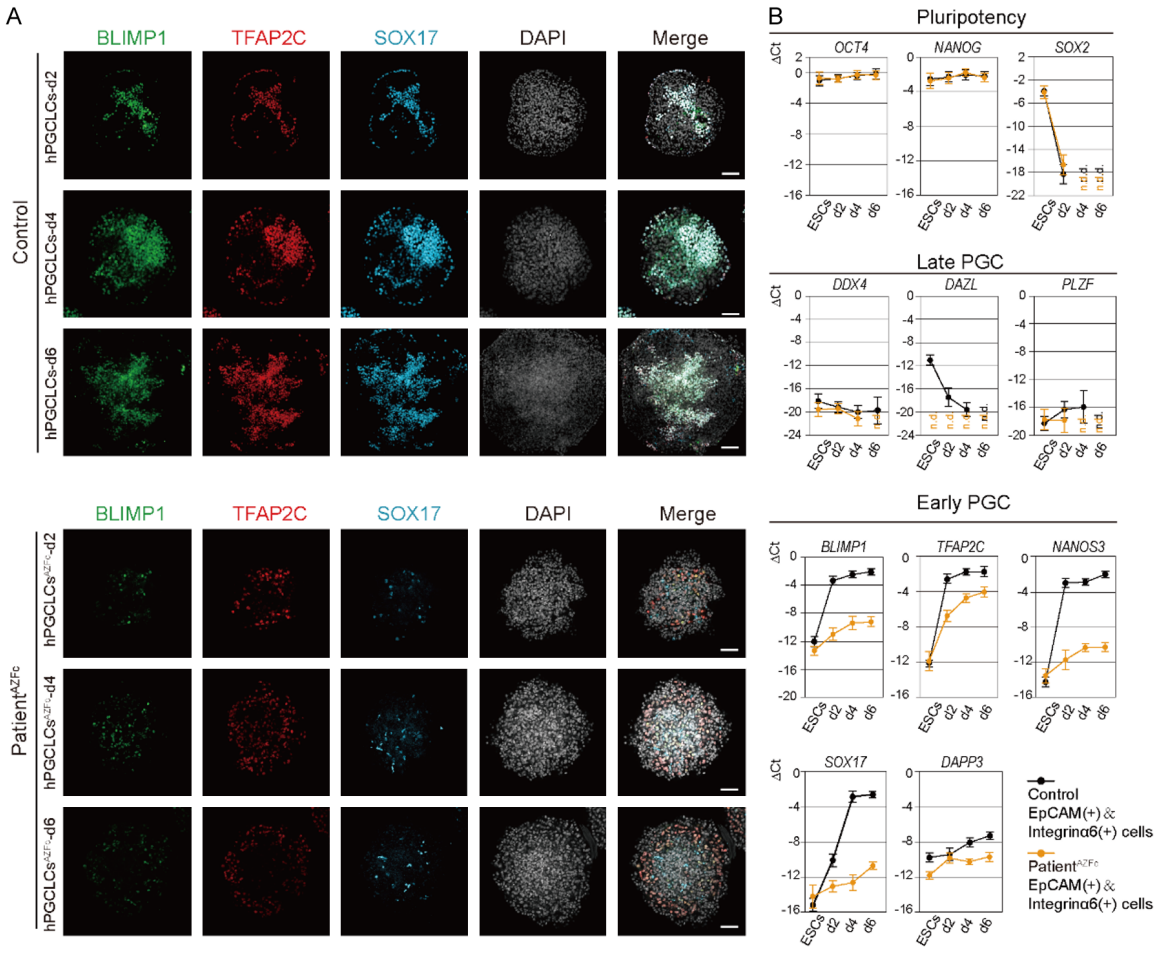

Figure 3. DAZ deficiency impairs critical transcription factor expression during hPGCLCs specification. A. Immunofluorescence analysis of germ cell transcription factors BLIMP1 (Green), TFAP2C (Red), and SOX17 (Cyan) in Control and PatientAZFc floating aggregates at Day 2/4/6. The DNA was stained with DAPI. Scale bar, 50 μm. B. Gene expression dynamics during the induction of CD326+ and CD49F+ cells were analyzed at days -2 (representing hESCs), day 2 (whole aggregates), and days 4 and 6 (CD326+ and CD49F+ cells) in the Control and PatientAZFc groups, as measured by qPCR. For each gene examined, the ΔCt (from the average Ct values of the housekeeping gene GAPDH, set as 0) was calculated and plotted for three independent experiments. Mean values are connected by a line; 'n.d.' indicates not detected.

mark of committed hPGCLCs-was significantly reduced in DAZ-deficient cultures compared to controls (**Figure 4J**).

Collectively, these findings demonstrate that DAZ deficiency confers a competitive advantage in clonal expansion but disrupts the normal identity of hPGCLCs. The combined morphological and flow cytometric evidence strongly indicates that DAZ-deficient hPGCLCs undergo dedifferentiation toward a pluripotent stem cell-like state.

Transcriptomic analysis identifies HMGA1 as a key regulator in DAZ-deficient cells

To identify the molecular mechanisms underlying the observed phenotypes, we performed RNA sequencing on H1 and SKLRMe001-A cells at different stages of hPGCLCs differentiation. Differential expression analysis identified 1,228 significantly altered genes (FDR < 0.01) between the two cell lines during differentiation (**Figure 5A**). Pathway enrichment analysis revealed significant changes in pathways related to cell cycle regulation, apoptosis, DNA damage response, and developmental processes. Among the differentially expressed genes, HMGA1, a key transcription factor, was significantly upregulated in SKLRMe001-A cells during hPGCLCs differentiation (**Figure 5B**).

HMGA1 expression in SKLRMe001-A cells was significantly higher than in H1 cells (FC > 2, P < 0.0001). Based on existing literature, HMGA1

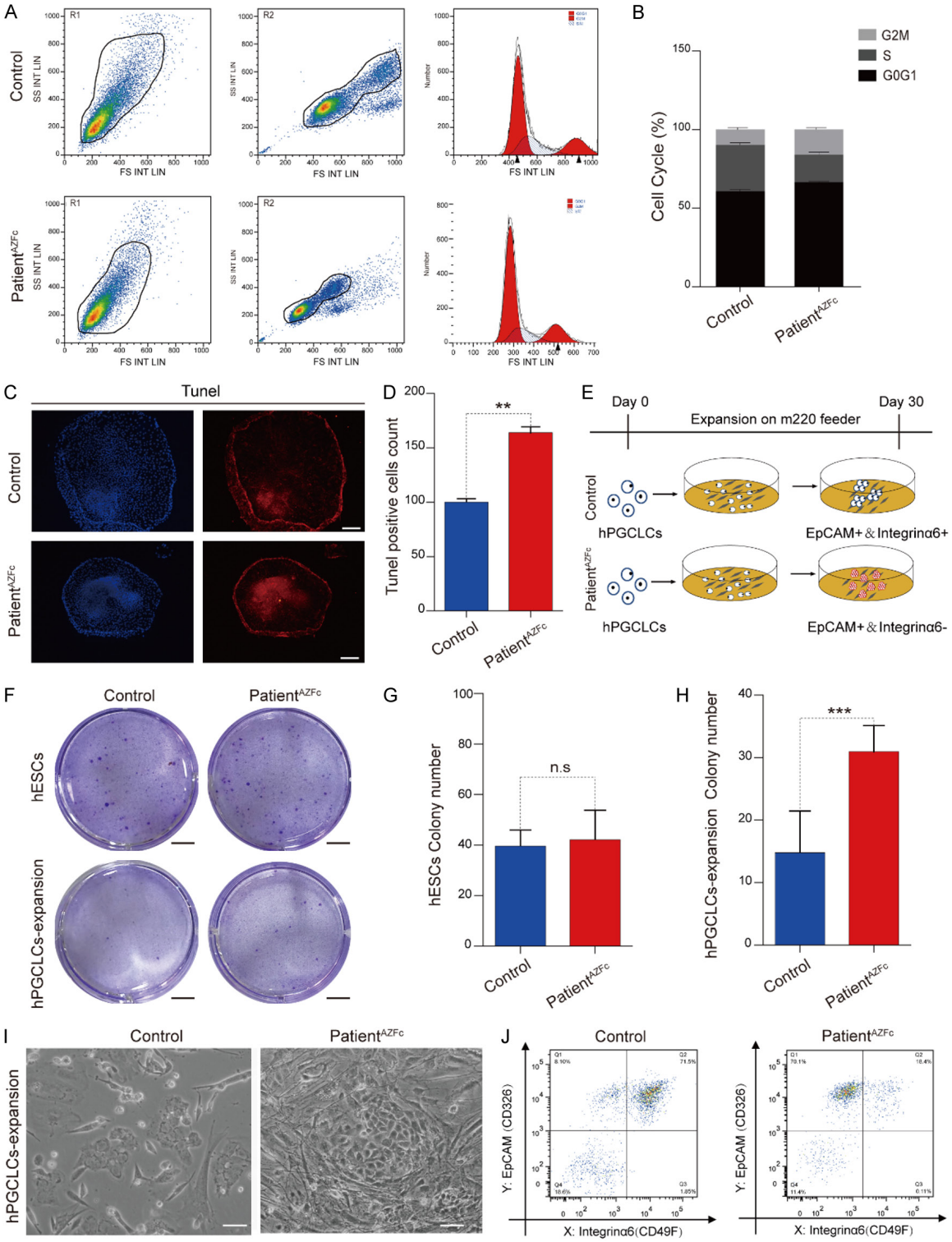

Figure 4. DAZ deficiency induces apoptosis in hPGCLCs differentiation and inhibits hPGCLCs expansion in vitro. A. Representative flow cytometric analysis of propidium iodide (PI)-stained cells showing cell cycle distribution in Control and PatientAZFc groups hPGCLCs at Day 4 of differentiation. B. Quantitative analysis reveals shortened S-phase, prolonged G0/G1, and delayed G2/M transition in Control and PatientAZFc groups hPGCLCs at Day 4 of differentiation. C. Representative immunofluorescence images of TUNEL (Red) and DAPI (Blue) staining in Control and PatientAZFc groups hPGCLCs at Day 6 of differentiation. The DNA was stained with DAPI. Scale bar, 50 μm. D. Quantification of TUNEL-positive cells per field (mean ± SEM, 3 independent experiments with ≥ 5 aggregates/

group). **P < 0.01 by unpaired t-test. E. Expansion of hPGCLCs (CD326+ and CD49F+ cells) on the m220 cells in the Control and PatientAZFc groups. Mean values are shown as bars. ***P < 0.001 by unpaired t-test. F. Crystal violet staining for the expansion of hESCs and hPGCLCs in Control and AZFc-deleted patient groups. G. hESCs colony number for control (blue) and PatientAZFc (red) groups. Data are from 6 independent experiments. Mean values are shown as bars. n.s (not significant), P > 0.05 by unpaired t-test. H. hPGCLCs-expansion Colony number for control (blue) and PatientAZFc (red) groups. Data are from 6 independent experiments. Mean values are shown as bars. Mean values are shown as bars. ***P < 0.001 by unpaired t-test. I. Bright-field (BF) images of hPGCLCs expansion on m220 cells at Day 10 for control and PatientAZFc groups. Scale bars: 20 μm. J. Flow cytometric analysis of EP-CAM (CD326) and Integrin-α6 (CD49F) expression during hPGCLCs expansion in Control and PatientAZFc groups.

expression dramatically decreases during the differentiation of human spermatogonia stem cells into mature cells. However, in this experiment, HMGA1 expression in SKLRMe001-A cells was significantly higher than in H1 cells and continued to increase with differentiation induction, suggesting that abnormally high HMGA1 expression may play a key role in early spermatogonia stem cell differentiation disorders.

Using the TRRUST online tool for transcriptional regulatory analysis, we predicted potential upstream regulatory genes that may regulate HMGA1 and downstream target genes that HMGA1 may regulate. As shown in **Figure 5C**, we identified two potential activating regulators of HMGA1: E2F1 and MYCN. The downstream genes that HMGA1 may directly regulate include one activating gene (TP53) and four inhibitory genes (BRCA1, CDH1, INSR, and XPA). These key upstream and downstream genes provide alternative directions for elucidating the regulatory mechanisms of HMGA1 in early spermatogonia stem cell differentiation disorders. Initial analysis of downstream target genes regulated by HMGA1 in the overall differentially expressed data revealed that these genes are enriched in GO functional events related to key regulatory events such as DNA transcription, DNA damage, cell proliferation, cell cycle, mitosis, and apoptosis (**Figure 5D**). For KEGG pathways, they are mainly enriched in signaling pathways such as TNF, NOD, NF-kappa B, PI3K, and MAPK (**Figure 5E**). Further considering the consistency of regulatory relationships, we found that upregulated downstream genes participate in the regulation of apoptosis, cell cycle, PI3K, and MAPK signaling pathways, while downregulated INSR, BRCA1, and CDH1, etc., participate in the regulation of adhesion, Rap1, and FoxO signaling pathways (**Figure 5F**).

Discussion

This study aimed to mechanistically link Y chromosome AZFc deficiencys encompassing the DAZ gene with male infertility and susceptibility to testicular germ cell tumors (TGCTs), utilizing a human embryonic stem cell (hESC)-based germline differentiation model. By directing DAZ-deleted hESC cell lines (SKLRMe001-A) and normal male hESC cell lines (H1) to differentiate into human primordial germ cell-like cells (hPGCLCs), the study demonstrated that DAZ deficiency impaired the ability of hESCs to differentiate into hPGCLCs, resulting in structurally fragile germ cell aggregates, disrupted cell cycle, and increased apoptosis. Transcriptomic analysis identified the chromatin architectural factor HMGA1 as a central transcriptional-signaling hub, and sustained HMGA1 upregulation may be associated with an undifferentiated, embryonic-like state, converging on the TP53 and PI3K/AKT-MAPK axes.

In recent years, breakthroughs have been made in the in vitro induction of primordial germ cells (PGCs) from pluripotent stem cells [14]. In mouse models, primordial germ cell-like cells (PGCLCs) induced from embryonic stem cells (ESCs) and induced pluripotent stem cells (iPSCs) can complete meiosis in vivo or in vitro to obtain artificial gametes and produce healthy offspring [20, 21]. In vitro germ cell specification from human pluripotent stem cells relies on a deep understanding of stem cell differentiation regulatory networks and PGC development. Surani et al. used human ESCs (hESCs) to specify human PGCLCs (hPGCLCs) in vitro to study the regulatory network of early human PGC (hPGC) specification [22, 23]. Saitou et al. through studies of human and non-human primate embryonic development, established culture methods for in vitro induction and expansion of early PGCLCs from human and non-human primate iPSCs [14-17, 24]. Studies have shown that although hPGCLCs are at an early stage of PGC development, the efficiency of in vitro induction of hPGCLCs from stem cells can still demonstrate differences in primordial germ cell differentiation [13, 14, 25].

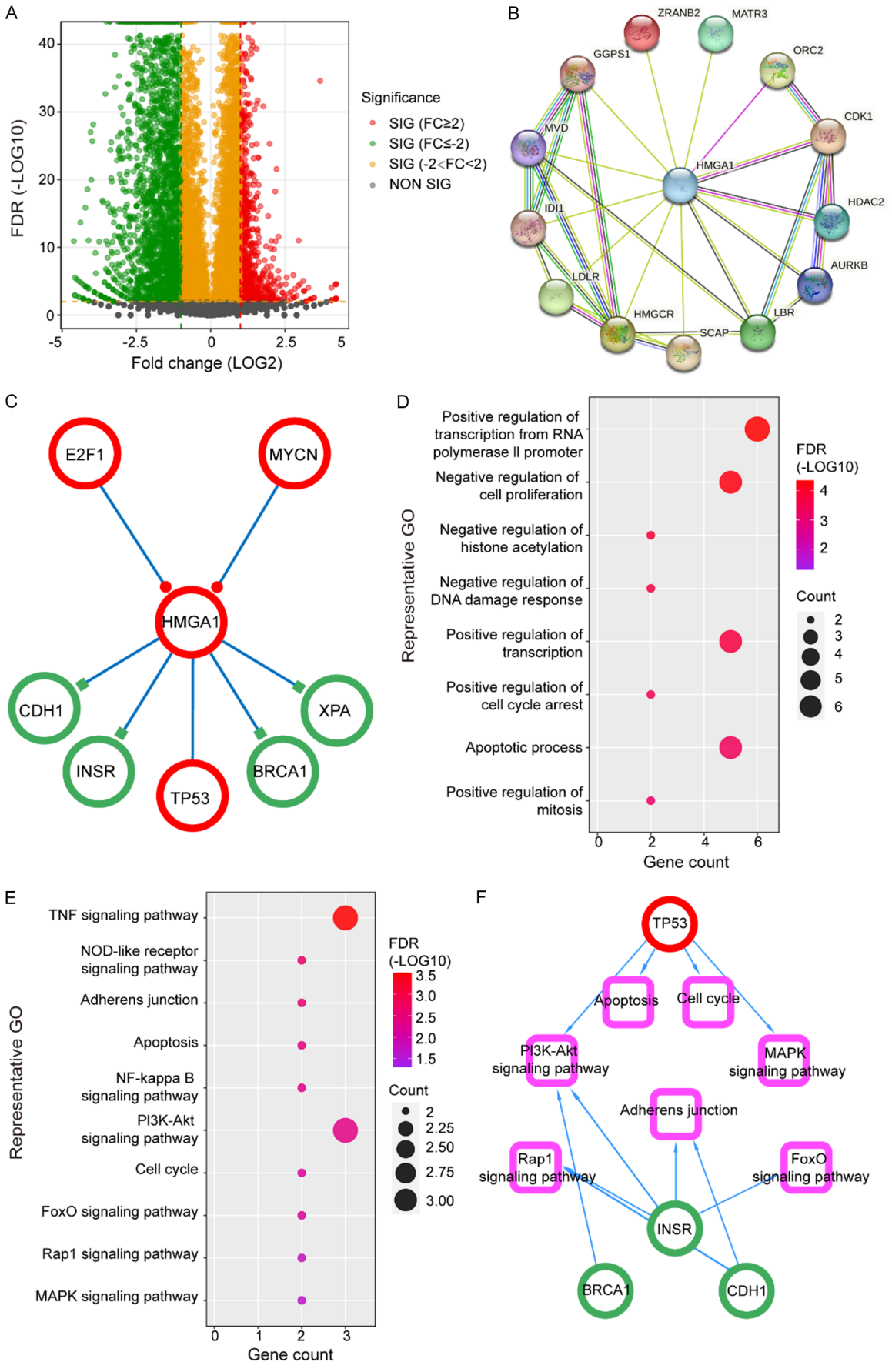
A
FDR (-LOG10)
Fold change (LOG2)
Significance
SIG (FC≥2)
SIG (FC≤-2)
SIG (-2<FC<2)
NON SIG
B
ZRANB2
MATR3
GGPS1
ORC2
CDK1
MVD
HMGA1
HDAC2
IDI1
AURKB
LDLR
HMGCR
LBR
SCAP
C
E2F1
MYCN
HMGA1
CDH1
XPA
INSR
TP53
BRCA1
D
Representative GO
Positive regulation of transcription from RNA polymerase II promoter
Negative regulation of cell proliferation
Negative regulation of histone acetylation
Negative regulation of DNA damage response
Positive regulation of transcription
Positive regulation of cell cycle arrest
Apoptotic process
Positive regulation of mitosis
Gene count
FDR (-LOG10)
Count
E
Representative GO
TNF signaling pathway
NOD-like receptor signaling pathway
Adherens junction
Apoptosis
NF-kappa B signaling pathway
PI3K-Akt signaling pathway
Cell cycle
FoxO signaling pathway
Rap1 signaling pathway
MAPK signaling pathway
Gene count
FDR (-LOG10)
Count
F
TP53
Apoptosis
Cell cycle
PI3K-Akt signaling pathway
MAPK signaling pathway
Adherens junction
Rap1 signaling pathway
FoxO signaling pathway
INSR
BRCA1
CDH1

Figure 5. Transcriptomic analysis identifies HMGA1 as a key regulator in DAZ-deficient cells. A. Relative to an expression volcano plot, the x-axis represents fold change, and the y-axis represents *p*-value. B. HMGA1 Core Regulatory Network Diagram. C. E2F1 and MYCN were identified as regulatory factors that influence the activation of HMGA1. Downstream genes directly regulated by HMGA1 include one activated gene (TP53) and four repressed genes (BRCA1, CDH1, INSR, and XPA). D. Differentially expressed genes are enriched in GO functional terms. E. Differential genes enriched in KEGG pathways. F. Key Regulatory Network Analysis.

To investigate the mechanism by which DAZ gene deficiency leads to spermatogenic disorders, we performed transcriptome sequencing analysis to identify differentially expressed genes between the two groups of cells. We found that SKLRMe001-A showed abnormalities during differentiation into early hogs, and the expression of the key gene HMGA1 was significantly activated, inhibiting early primordial germ cell (PGC) differentiation, suggesting that abnormal high expression of HMGA1 may play a key role in primordial germ cell differentiation disorders. We further used the TRRUST online transcription regulation analysis tool to predict and analyze potential upstream regulatory genes of HMGA1 and downstream target genes regulated by HMGA1. HMGA1 may be a key transcription regulator in the process of stem cell differentiation. We speculate that when DAZ deficiency leads to abnormal high expression of HMGA1, it activates the P53 gene and, through the downstream MAPK/PI3K signaling pathway, leads to apoptosis and cell cycle abnormalities, ultimately causing early germ cell differentiation disorders.

HMGA1, as a key transcription factor, is widely distributed in the nuclei of higher eukaryotic cells and plays an important role in the growth, development, cell proliferation, and differentiation of higher eukaryotes [26]. It is widely involved in a variety of important intranuclear biological functions, including regulation of DNA replication, transcription, recombination, and repair [27]. In addition, it has been reported that HMGA1 and HMGA2 are highly expressed in Sertoli cells, spermatogonia, and spermatocytes within normal adult mouse testicular tissue, suggesting that HMGA1 and HMGA2 may participate in the division, proliferation, and spermatogenesis of normal male mouse spermatogenic epithelial cells [28]. Recently, single-cell RNA sequencing (scRNA-seq) of testicular cells from 2854 normospermic donors and 174 testicular cells from one NOA donor identified several stage-specific marker genes of human germ cells and found that HMGA1 is actively transcribed in spermatogonia located near the basal lamina of the seminiferous epithelium and gradually downregulated in other spermatogenic cells [29]. Our conclusions are consistent with existing research and also demonstrate that the differentiation defect of the DAZ-deleted embryonic stem cell line into hPGCLCs is related to abnormal HMGA1 expression.

HMGA1 is frequently overexpressed in various male-related tumors and is generally associated with tumor invasion, metastasis, drug resistance, and poor prognosis [30]. HMGA1 can enhance the migration and drug resistance of tumor cells by promoting the expression of AR (androgen receptor) signaling downstream genes, driving EMT, regulating miRNAs, and activating pathways such as PI3K/AKT and Wnt/β-catenin [31, 32]. Concurrently, HMGA family proteins are often highly expressed in embryonal-like tumors or germ cell tumors, correlating with the undifferentiated state and stem cell-like characteristics of the tumors [33].

This study has several limitations that need to be addressed in future research. First, although our in vitro model recapitulates the early stages of germ cell development, it does not fully reflect the complexity of in vivo spermatogenesis.

Second, although we have identified HMGA1 as a key mediator, the specific mechanism by which DAZ deficient leads to HMGA1 upregulation needs further clarification. Despite these limitations, our study significantly advances the understanding of the function of DAZ protein in human germ cell development and its implication in the development of germ cell developmental abnormalities and testicular germ cell tumors (TGCTs).

Conclusions

This study, utilizing a specific human embryonic stem cell (hESC) model, constructed and char-

acterized a DAZ-deficient cell line. The results demonstrate that DAZ deficiency significantly weakens the efficiency of hPGCLC induction, inhibits the expression of key early germline lineage factors (SOX17, BLIMP1, TFAP2C), and is accompanied by shortened S phase, cell cycle imbalance, and increased apoptosis. Transcriptomic and enrichment analyses revealed sustained upregulation of HMGA1 and dysregulation of P53 stress and the PI3K/AKT and MAPK signaling pathways, indicating the maintenance of an embryonic-like program, activation of proliferation signals, and enhanced DNA damage response, consistent with testicular germ cell tumors (TGCTs). Based on these findings, we propose that DAZ deficiency-induced lineage differentiation defects and "stress-survival" signal mismatch may lead to the formation of an "undifferentiated and susceptible" cell population in vivo, thereby simultaneously increasing TGCT risk and elucidating the developmental basis of male infertility. HMGA1 was identified as a central transcriptional-signaling hub, providing molecular clues for risk stratification and early monitoring of individuals carrying DAZ deficiencys, and suggesting that interventions targeting HMGA1 and the PI3K/AKT and MAPK pathways may improve germline differentiation while reducing potential tumor risk.

Acknowledgements

The authors thank the members of the Yan Yuan laboratory and the Jiahao Sha laboratory for their technical assistance and helpful comments. This work was supported by Science Foundation of Jiangsu Province (BK20240725), National Natural Science Foundation of China (No. 32400948), grants from the Training plan of National Nature and Science Foundation of China (PY2022013), the 2023 Outstanding Young Doctor Training Project (Grant No. 2023QB0141).

Disclosure of conflict of interest

None.

Address correspondence to: Dr. Feiyang Diao, Clinical Center of Reproductive Medicine, First Affiliated Hospital of Nanjing Medical University, Nanjing Medical University, Nanjing 210029, Jiangsu, China. E-mail: phenix_y@163.com; Xingli Tong, Jiangsu Province Hospital of Chinese Medicine, Affiliated Hospital of Nanjing University of Chinese, Nanjing 210000, Jiangsu, China. E-mail: 18651857662@163.com

References

[1] Matsumoto D, Mizuno K, Nishio H, Kamisawa H, Sakata T, Kato T, Nakane A, Kurokawa S, Maruyama T, Hayashi Y and Yasui T. Effects of neonatal hypothyroidism on testicular development and undifferentiated spermatogonia in prepubertal rats. Andrology 2025; [Epub ahead of print].

[2] Colaco S and Modi D. Genetics of the human Y chromosome and its association with male infertility. Reprod Biol Endocrinol 2018; 16: 14.

[3] Koh E, Sin HS, Fukushima M and Namiki M. Azoospermia factor and male infertility. Reprod Med Biol 2010; 9: 129-137.

[4] Gromoll J, Weinbauer GF, Skaletsky H, Schlatt S, Rocchietti-March M, Page DC and Nieschlag E. The old world monkey DAZ (Deleted in AZoospermia) gene yields insights into the evolution of the DAZ gene cluster on the human Y chromosome. Hum Mol Genet 1999; 8: 2017-2024.

[5] Saunders PT, Turner JM, Ruggiu M, Taggart M, Burgoyne PS, Elliott D and Cooke HJ. Absence of mDazl produces a final block on germ cell development at meiosis. Reproduction 2003; 126: 589-597.

[6] Simonik O, Bryndova B, Sur VP, Ded L, Cockova Z, Benda A, Qasemi M, Pecina P, Pecinova A, Spevakova D, Hradec T, Skrobanek P, Ezrova Z, Kratka Z, Kren R, Jeseta M, Boublikova L, Zamecnik L, Buchler T, Neuzil J, Postlerova P and Komrskova K. Bioenergetics of human spermatozoa in patients with testicular germ cell tumours. Mol Hum Reprod 2025; 31: gaaf005.

[7] Qasemi M, Sur VP, Simonik O, Postlerova P, Skrobanek P, Hradec T, Boublikova L, Zamecnik L, Buchler T, Neuzil J and Komrskova K. Sperm mitochondria dysfunction in response to testicular cancer. Eur J Clin Invest 2024; 54: e14146.

[8] Choi H and Cheon YP. Anatomy and function of deleted in azoospermia like (DAZL) gene in human and mouse. Dev Reprod 2025; 29: 19-30.

[9] Xu EY, Lee DF, Klebes A, Turek PJ, Kornberg TB and Reijo Pera RA. Human BOULE gene rescues meiotic defects in infertile flies. Hum Mol Genet 2003; 12: 169-175.

[10] Lin Y and Page DC. Dazl deficiency leads to embryonic arrest of germ cell development in XY C57BL/6 mice. Dev Biol 2005; 288: 309-316.

[11] Wang M, Liu X, Chang G, Chen Y, An G, Yan L, Gao S, Xu Y, Cui Y, Dong J, Chen Y, Fan X, Hu Y, Song K, Zhu X, Gao Y, Yao Z, Bian S, Hou Y, Lu J, Wang R, Fan Y, Lian Y, Tang W, Wang Y, Liu J, Zhao L, Wang L, Liu Z, Yuan R, Shi Y, Hu B, Ren X, Tang F, Zhao XY and Qiao J. Single-Cell RNA sequencing analysis reveals sequential cell

fate transition during human spermatogenesis. Cell Stem Cell 2018; 23: 599-614, e4.
[12] De Felici M, Klinger FG, Campolo F, Balistreri CR, Barchi M and Dolci S. To be or not to be a germ cell: the extragonadal germ cell tumor paradigm. Int J Mol Sci 2021; 22: 5982.
[13] Hancock GV, Wamaitha SE, Peretz L and Clark AT. Mammalian primordial germ cell specification. Development 2021; 148: dev189217.
[14] Saitou M and Hayashi K. Mammalian in vitro gametogenesis. Science 2021; 374: eaaz6830.
[15] Sasaki K, Yokobayashi S, Nakamura T, Okamoto I, Yabuta Y, Kurimoto K, Ohta H, Moritoki Y, Iwatani C, Tsuchiya H, Nakamura S, Sekiguchi K, Sakuma T, Yamamoto T, Mori T, Woltjen K, Nakagawa M, Yamamoto T, Takahashi K, Yamanaka S and Saitou M. Robust in vitro induction of human germ cell fate from pluripotent stem cells. Cell Stem Cell 2015; 17: 178-194.
[16] Murase Y, Yokogawa R, Yabuta Y, Nagano M, Katou Y, Mizuyama M, Kitamura A, Puangsricharoen P, Yamashiro C, Hu B, Mizuta K, Tsujimura T, Yamamoto T, Ogata K, Ishihama Y and Saitou M. In vitro reconstitution of epigenetic reprogramming in the human germ line. Nature 2024; 631: 170-178.
[17] Murase Y, Yabuta Y, Ohta H, Yamashiro C, Nakamura T, Yamamoto T and Saitou M. Long-term expansion with germline potential of human primordial germ cell-like cells in vitro. EMBO J 2020; 39: e104929.
[18] Li C, Cai L, Dong J, Ning S, Zhou J, Wu H, Cui Y, Qin L and Yang X. Establishment of human embryonic stem cell (SKLRMe001-A) carrying Azoospermic factor c (AZFc) deficiencys. Stem Cell Res 2022; 59: 102625.
[19] Sybirna A, Wong FCK and Surani MA. Genetic basis for primordial germ cells specification in mouse and human: conserved and divergent roles of PRDM and SOX transcription factors. Curr Top Dev Biol 2019; 135: 35-89.
[20] Zhou Q, Wang M, Yuan Y, Wang X, Fu R, Wan H, Xie M, Liu M, Guo X, Zheng Y, Feng G, Shi Q, Zhao XY, Sha J and Zhou Q. Complete meiosis from embryonic stem cell-derived germ cells in vitro. Cell Stem Cell 2016; 18: 330-340.
[21] Ishikura Y, Ohta H, Sato T, Murase Y, Yabuta Y, Kojima Y, Yamashiro C, Nakamura T, Yamamoto T, Ogawa T and Saitou M. In vitro reconstitution of the whole male germ-cell development from mouse pluripotent stem cells. Cell Stem Cell 2021; 28: 2167-2179, e2169.
[22] Irie N, Lee SM, Lorenzi V, Xu H, Chen J, Inoue M, Kobayashi T, Sancho-Serra C, Drousioti E, Dietmann S, Vento-Tormo R, Song CX and Surani MA. DMRT1 regulates human germline commitment. Nat Cell Biol 2023; 25: 1439-1452.
[23] Irie N, Weinberger L, Tang WW, Kobayashi T, Viukov S, Manor YS, Dietmann S, Hanna JH and Surani MA. SOX17 is a critical specifier of human primordial germ cell fate. Cell 2015; 160: 253-268.
[24] Yamashiro C, Sasaki K, Yabuta Y, Kojima Y, Nakamura T, Okamoto I, Yokobayashi S, Murase Y, Ishikura Y, Shirane K, Sasaki H, Yamamoto T and Saitou M. Generation of human oogonia from induced pluripotent stem cells in vitro. Science 2018; 362: 356-360.
[25] Kojima Y, Sasaki K, Yokobayashi S, Sakai Y, Nakamura T, Yabuta Y, Nakaki F, Nagaoka S, Woltjen K, Hotta A, Yamamoto T and Saitou M. Evolutionarily distinctive transcriptional and signaling programs drive human germ cell lineage specification from pluripotent stem cells. Cell Stem Cell 2017; 21: 517-532, e515.
[26] Zhao Y, Liu MJ, Zhang L, Yang Q, Sun QH, Guo JR, Lei XY, He KY, Li JQ, Yang JY, Jian YP and Xu ZX. High mobility group A1 (HMGA1) promotes the tumorigenesis of colorectal cancer by increasing lipid synthesis. Nat Commun 2024; 15: 9909.
[27] He KY, Zhao A, Guo JR, Wu DH, Liu H, Gao F, Liu MJ, Yang JY, Lei XY, Li JQ, Zhang L, Yan ZH, Ding Q, Huang YW, Cui R, Jian YP and Xu ZX. High mobility group A1 (HMGA1) promotes esophageal squamous cell carcinoma progression by inhibiting STING-mediated anti-tumor immunity. Nat Commun 2025; 16: 5098.
[28] Esposito F, Boscia F, Gigantino V, Tornincasa M, Fusco A, Franco R and Chieffi P. The high-mobility group A1-estrogen receptor beta nuclear interaction is impaired in human testicular seminomas. J Cell Physiol 2012; 227: 3749-3755.
[29] Ou N, Wang Y, Xu S, Luo J, Zhang C, Zhang Y, Shi X, Xiong M, Zhao L, Ji Z, Zhang Y, Zhao J, Bai H, Tian R, Li P, Zhi E, Huang Y, Chen W, Wang R, Jin Y, Wang D, Li Z, Chen H and Yao C. Primate-specific DAZ regulates translation of cell proliferation-related mRNAs and is essential for maintenance of spermatogonia. Adv Sci (Weinh) 2024; 11: e2400692.
[30] Zhang L, Zhao X, Gao X, Qin H, Chen F and Lin Z. Complicated crosstalk between HMGA and non-coding RNAs modulates hallmarks of cancer. Cancer Cell Int 2025; 25: 80.
[31] Liu X, Zhang X, Zeng T, Chen Y, Ye L, Wang S and Li Y. FOSL1 drives the malignant progression of pancreatic cancer cells by regulating cell stemness, metastasis and multidrug efflux system. J Transl Med 2025; 23: 268.

[32] Luo LZ, Kim JH, Herrera I, Wu S, Wu X, Park SS, Cho J, Cope L, Xian L, West BE, Calderon-Espinosa J, Kim J, Thompson Z, Maloo I, Larman T, Reddy KL, Feng Y, Fearon ER, Sears CL and Resar L. HMGA1 acts as an epigenetic gatekeeper of ASCL2 and Wnt signaling during colon tumorigenesis. J Clin Invest 2025; 135: e184442.

[33] Zhang Y, Xiao Y, Zhao X, Xu J, Zhao H, Guo Z, Zhao J, Zhang Y, Wang R and Wang J. IGF2BP3 is upregulated in endometrial cancer and tightly regulates the growth of drug-resistant endometrial cancer cells via HMGA1. Sci Prog 2025; 108: 368504251315008.